Low Dye Content Efficient Dye-Sensitized Solar Cells using Carbon Doped-Titania Paste from convenient Green Synthetic Process

Riccardo Momoli,[a] Alessandro Gandin,[a,b] Riccardo Ruffo,[c,d] Samiha Chaguetmi,[e] Fayna Mammeri,[e] Alessandro Abbotto, [c,d*] Norberto Manfredi,[c,d*] and Giovanna Brusatin[a,b *]

[a] Industrial Engineering Department University of Padova, via Marzolo 9, 35131 Padova (Italy)

[b] INSTM Unit of University of Padova, Via Marzolo 9, 35131 Padova (Italy)

[c] Department of Materials Science and Milano-Bicocca Solar Energy Research Center - MIB-Solar, University of Milano-Bicocca, Via Cozzi 55, I-20125 Milano (I)

[d] INSTM Unit of University of Milano-Bicocca, Via Cozzi 55, I-20125 Milano (I)

[e] Université de Paris, ITODYS, CNRS, F-75006 Paris, France.

KEYWORDS: Titanium dioxide; Dye-sensitized solar cell; green synthesis; C-doped TiO_2; sugar

This paper is dedicated to the Memory of the late Professor Renato Ugo, great scientist and teacher.

ABSTRACT: In this paper, we present a green approach based on a simple "multi-step" mild process to easily produce carbon doped TiO_2, using low-cost titania nanoparticles and chemical eco-friendly glucose ($C_6H_{12}O_6$) as the C-dopant. DSSCs produced by C-doped samples show increased visible light absorption. Using a single 12 μm layer, the C-doped photoanode reached the same solar energy conversion efficiency obtained by the photoanode film prepared from conventional TiO_2 nanoparticles but using half of dye content, as a consequence of improved electronic performances.

1. Introduction

Since the initial work by Graetzel and O'Regan in 1991[1] and the fabrication of the first photovoltaic (PV) prototype, dye-sensitized solar cells (DSSC) have attracted much attention, allowing to forecast a slow but steady growth of the DSSC market up to 2023.[2],[3] In particular, the scientific research is focusing on the optimization of every single components of the device,[4-9] with the aim of improving the power conversion efficiency (PCE) and long-term stability of the cell and simplifying the industrialization process towards a valid alternative to the silicon based PV technology. Titanium dioxide (TiO_2) has been extensively used as the photoanode n-type semiconductor, thanks to its low-cost, long-term stability, and non-toxicity. However, the main drawback of the use of TiO_2 lies in its intrinsic wide bandgap (3.2 eV), thus directly harvesting only 3-5% of the solar radiation. The strategies adopted for improving the harvesting efficiency of TiO_2 can be summarized as either morphological modifications, such as higher surface area and porosity, or as chemical modifications, by incorporation of additional components in the TiO_2 structure. Accordingly, many efforts have been dedicated to develop TiO_2-based materials that could bridge both the UV (290-400 nm) and the visible (400-700 nm) radiation and reduce the recombination of electron/hole pairs, thereby enhancing the overall absorption efficiency.[10]

Attempts toward achieving this goals have relied, in part, on photosensitizing the metal oxide by molecular visible-light-harvesters, such as suitable organic dyes [11, 12] and suitable metal-ion dopants.[13, 14] However, both approaches present serious drawbacks. Although organic dyes allowed DSSC record efficiencies,[15, 16] often undergo natural degradation thus permitting limited long-term stability under light soaking and thermal stress. On the other hand, metal dopants act as recombination centres for the photogenerated charge carriers. To overcome these limitations, researchers started to consider nonmetals-doping (N, C, S and F) as a prelude to increase the photoactivity of this metal,[17] following the pioneering work of Asahi et al. in 2001.[18]

Visible-light activation of TiO_2 specimens (anion-doped or otherwise) have been attributed either to defects associated with oxygen vacancies that give rise to color centres[17, 19] or to a narrowing of the original band-gap of TiO_2 through mixing of dopant and oxygen 2p orbitals.[18] Nevertheless, the chemical nature of the doped species, responsible for the visible titania photoactivity, and the electronic structure of the doped material have not been yet fully exploited.[20]

Among the anionic dopant, carbon [21-23] and nitrogen[24-26] are the most employed and are introduced into the titania structure in concentration ranging parts per thousand to parts per hundreds. The effects and the efficiency of doping greatly vary with the employed techniques and synthetic methods. A common observation among the studied techniques is the creation of localized extrinsic energy levels inside the band-gap of TiO_2.[27] The optical transitions between these levels and the Ti 3d levels (which are the main component of the CB edge), are responsible for the improve in the absorption properties of the material, and are traced by the shift of absorption threshold of TiO_2 in the form of shoulders or tails towards higher wavelength range of the radiation.

Aiming to overcome the current limits of DSSC and reach a higher PCE, this work investigates the device performances using easily obtainable and low cost carbon-doped TiO_2, synthesized through a sustainable and easily scalable chemical route, ready for fast industrialization. Intensive efforts have been made so far to develop methods for synthesizing nonmetal-doped TiO_2-based photocatalysts. The three most important methods for the synthesis of C-doped TiO_2 are: 1. high-temperature sintering of carbon-containing TiO_2 precursor, 2. CVD or pyrolysis, 3. solution-phase strategies.[28-36] Most of the methods require high-temperature treatments (400-850 °C), use expensive, toxic, or unstable precursors, and are tedious to conduct, making difficult a large-scale application. Therefore, it is of particular importance to develop a facile, energy efficient, and environmentally friendly approach for the synthesis of C-doped TiO_2 nanomaterials with high visible photocatalytic activity.

Other synthetic routes, such as simple wet chemistry techniques, can solve the aforementioned issues. These approaches rely on its efficiency to afford pure products while minimizing the number of preparation steps and avoiding the use of either excessively harmful reagents or unstable precursors, with no generation of toxic by-products. Thus, such a method is efficient in scale-up procedures and benign to human health and the environment.

In our previous work in collaboration with Professor Ugo's group, we observed an enhancement of the photovoltaic performances in DSSCs using novel organometallic dyes as sensitizers adsorbed over a photoanode based on C-doped TiO_2.[37] To further investigate this positive phenomenon, we have thus investigated different C-doped TiO_2 anodes to point out its contribution to the overall device efficiency. In this contribution, we also present the green approach based on a simple "multi-step" mild process, where low-cost titania nanoparticles, and glucose ($C_6H_{12}O_6$) as the C-dopant, are used.[38] The obtained carbon doped titania pastes for DSSC exhibited significant enhancements of open-circuit voltage leading to a very performing cell exhibiting efficiency compared to the device using a photoanode film prepared from undoped anatase TiO_2 nanoparticles but using a smaller amount of sensitizer.

2. EXPERIMENTAL SECTION

2.1 Materials and methods

The following materials were purchased from commercial suppliers: FTO-coated glass plates (2.2 mm thick; sheet resistance ~7 ohm per square; Solaronix); TiO_2 (Solaronix Ti-Nanoxide T/SP 15–20 nm anatase particles for transparent sintered layers; Solaronix Ti-Nanoxide R/SP >100 nm TiO_2 particles for scattering sintered layers; Dyesol 18NR-AO active opaque TiO_2 blend of active 20 nm anatase particles and up to 450nm anatase scatter particles); and N719 (Sigma-Aldrich). UV-O_3 treatment was performed using Novascan PSD Pro Series – Digital UV Ozone System.

2.2 Synthetic procedure for C-doped Titania

The C-doped TiO_2 nanoparticles have been prepared varying the amount of glucose according to a previously reported procedure.[37]

2.3 General procedure for the preparation of the TiO_2 pastes

The preparation of TiO_2 pastes roots in the optimization of published procedures.[39, 40]

2.4 Preparation of DSSCs.

A scheme of the structure of the DSSC device is depicted in Figure 1.
DSSCs have been prepared according to a procedure reported in the literature.[39, 41]

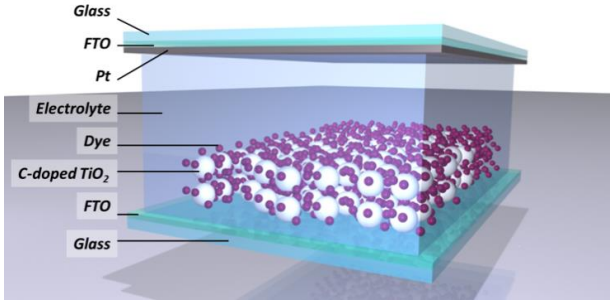

Figure 1. Scheme of a Dye-Sensitized Solar Cells (DSSC) obtained with doped TiO_2 paste

2.5 Dye loading

The amount of adsorbed dye has been measured for each sample as described in a previous manuscript.[42]

2.6 Characterization

The thickness, the optical properties and the photovoltaic performances have been evaluated according to the literature.[43]
The surface chemical composition of as prepared and functionalized NPs has been checked according to our previously published reports. [44]
Electrochemical Impedance Spectroscopy (EIS) measurements were performed according to the literature. [45, 46]
Photoelectrochemical techniques were carried out in a three-electrode configuration with the sample as working electrode, Pt rod as counter electrode and saturated calomel electrode as reference electrode (Figure 2). An aqueous solution of Na_2SO_4 0,5 M (pH 7) was used as electrolyte. Before the experiment, the solution was purged with argon in order to remove the dissolved oxygen.

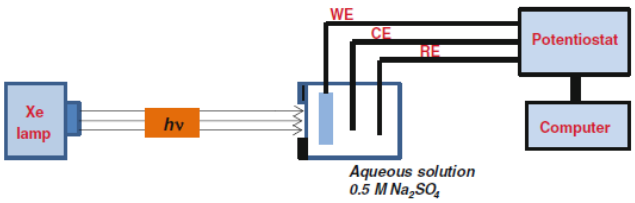

Figure 2: Scheme of the home-made Photoelectrochemical cell (PEC) in which CE, WE and RE correspond to the counter-electrode (Pt), working electrode (TiO_2) and the reference electrode (SCE) respectively.

A 150 W Xenon short-arc XBO lamp equipped with a AM 1.5 G filter was used as illumination source for simulate the solar light. For these tests we employed a quartz cell specifically designed with a window of 70 mm^2 area. The window was necessary for illuminating a controlled and constant portion of the sample. The lamp was positioned at a fixed distance (30 cm) from the cell and the lamp's power fixed at 150 W. Two different tests were carried out: cyclic voltammetry and chronoamperometry in order to check and monitor the photosensitization of the TiO_2 doped samples.

3. RESULTS AND DISCUSSION

3.1 C-doped Titania powder synthesis

The C-doped titania powder is prepared starting from abundant, cheap and environmentally friendly materials such as titanium dioxide, in our case pure anatase TiO_2, sugar and water. The procedure occurs in two steps, at relatively low temperatures compared to that used in common solution-phase strategies.[34-36] A suspension of TiO_2 is stirred for several hours at 85 °C with the proper amount of carbon source and then air dried, washed with water and dried again. The final material is achieved after grinding the so obtained power and a second thermal treatment at 225 °C.

3.2 Titania powder characterization

A detailed quantitative analysis of the electronic state of a sample was allowed by XPS (X-Ray Photoelectron Spectroscopy). The photoemission peaks depend on the chemical environment of the atoms from which they generate, and a shift is observable from the unperturbed atomic value if the chemical surrounding in changed. An extensive literature research did not present a univocal interpretation of XPS data regarding the assignment of the dopant peaks and the effectiveness of the doping treatment for TiO_2 nanoparticles. Notwithstanding, some signals are clear and unanimously assigned to the dopant we have employed in this work. The peak relative to the C 1s orbital extends for an interval in binding energy between 281-291 eV and many contributions can be recognized. The signals are assigned as follow: 281.8 eV is the Ti-C bond, 284.6 eV is the C-C bond and 288.6 eV are the Ti-O-C structures. Unfortunately, as it can be seen in Figure 3, one should remember the ubiquitous carbon contamination present on the top of any sample. In this sense, with our preliminary data, it is unreliable any conclusion about the signal of doping atoms as it was difficult to separate the contribution from adventitious carbon contamination.

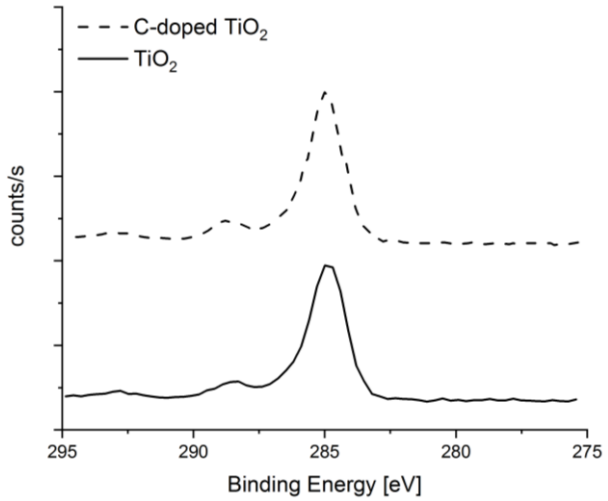

Figure 3. Comparison of the C 1s XPS signal of the samples.

Finally, XPS spectra of both undoped and doped titania, in Figure 4, exhibit two main contributions corresponding to Ti 2p3/2 and 2p1/2 at 458.5 - 458.7 eV and 464.4 eV, respectively, in good agreement with the previously reported XPS data on Ti^{4+}-based oxides.[47]

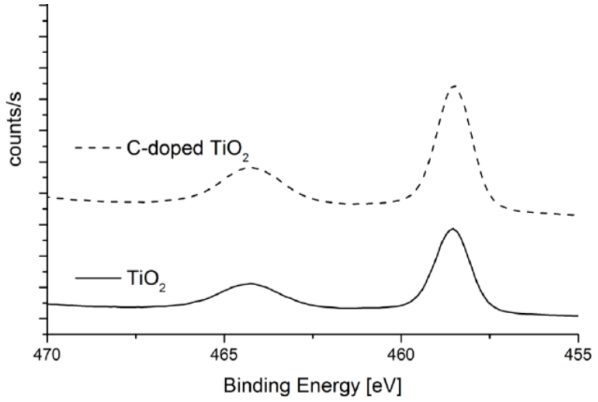

Figure 4. Comparison of the Ti 2p XPS signal of the samples.

Figure 5 shows the crystalline properties of the undoped and C-doped titania powders. The samples exhibit both anatase and rutile phase typical of Degussa P25 titania. Therefore, the doping of the particles didn't stain or distort the titania lattice properties. For the undoped P25 nanoparticles, the peaks indicate a 20 nm size for the anatase structure and 29 nm for the rutile structure. The C-doped sample show a slight increase in the crystal dimension, measuring 22 nm and 34 nm for the anatase and rutile phase, respectively.

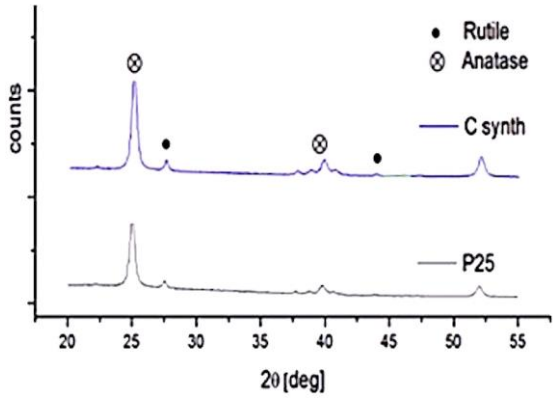

Figure 5. XRD analysis C-doped and undoped P25 titania

3.3 Titania paste characterization

The morphology of anodic samples deposited on glass substrate was evaluated through SEM analysis. As a great part of the electronic transport properties of the anode is given by its morphology, not only a smoother texture allows for longer migrating distances and efficient separation of couples, but also a greater surface area allow for a more efficient loading of the dye, thus in general increasing the power density of the cell. Moreover, pore size and distribution should be as smooth as possible, since rougher morphology reduces available surface area.

As reported in Figure 6, which show the TiO_2 electrode surface morphology obtained during doctor blade preparatory technique, there is no drastic change in the texture or porosity among the samples, both in the native P25 TiO_2 nanoparticles and in the C-doped samples. This allow us to conclude that the proposed strategy, given its lower process temperature as compared to other doping methods, such as flame pyrolysis, do not modify the aggregation state of the nanoparticles which are thus suitable for the preparation of the anodic material.

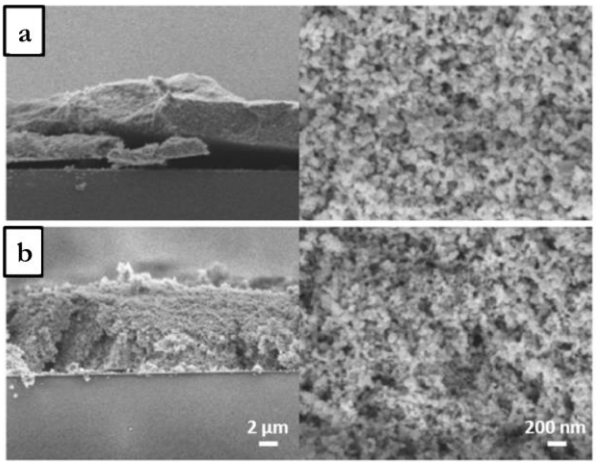

Figure 6. SEM images of the TiO_2 pastes deposited with doctor blade technique. (a) Carbon-doped TiO_2; (b) P25.

Photoelectrochemical properties of TiO_2 based films were evaluated through the study of cyclic voltammetry and chronoamperometry, using a homemade PEC cell. All photoanodes were illuminated intermittently at a given potential for several cycles, which led to an instantaneous change in current upon illumination. The current retracted to the original values almost instantaneously once the illumination is switched off. Several cycles were performed for each sample, for a potential of 0 V bias versus SCE.

Cyclic voltammetry was performed both in the dark and under simulated solar light to characterize the ability of the samples for PEC cells, through the measurement of J–E curves. All electrodes led to negligible current under dark conditions. Under illumination, the carbon doped sample exhibited a great enhancement of the current density compared to those of bare TiO_2 (P25) (Figure 7); a shift in onset potential of about 0.4 V was observed, suggesting a shift in Fermi level to more negative potential as a result of the introduction of carbon. The potential range of the measure is from -0.6 V to 0.6 V and the potential increasing rate is equal to 10.0 mV/s. The experimental current is plotted as a function of the applied voltage giving a voltammogram curve. To test the suitability of these samples for photoelectrochemical cell these measurements were done both in dark and under simulated solar light illumination conditions. We observed an increase of the photocurrent under illumination and for the doped sample. A higher photocurrent would one of the strategies to have a higher efficiency of the DSSC.

Chronoamperometry is an electrochemical technique in which the potential between the working electrode and the reference electrode is maintained constant and the current is measured as a function of time. Upon illumination the photo-induced separation of the electron-hole pairs led to a relatively large photocurrent peak. Then, the decrease of the photocurrent indicates that recombination of the electron-hole pairs occurs. The charge trap sites may be formed by crystal defects, such as Ti^{3+} in the TiO_2 surface, site impurities, surface amorphous layer and chemical surroundings. The traps would mainly be located on the surface of the particles, because of the high surface/volume ratio in nanosized system. Charge carriers which are generated deep inside the film take a longer time to reach the surface than those generated close to the surface, consequently they are more probably lost for recombination. The degree of the recombination with respect to the generation of the electron-hole pairs determines the rate of the photocurrent decay. A stable current is achieved once the charge generation and recombination reach the equilibrium.[48]

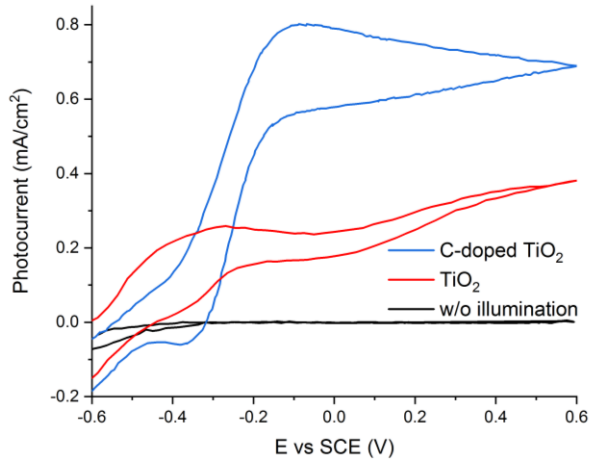

Figure 7. Cyclic voltammetry for C-TiO_2, TiO_2, and dark condition for the sample anodes.

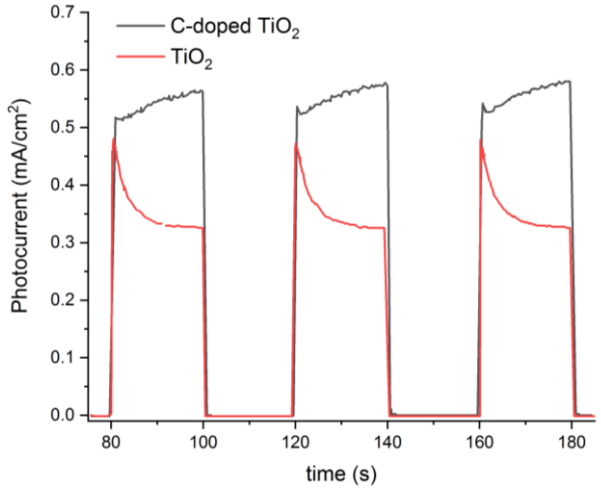

Figure 8. Photocurrent responses in Na_2SO_4 aqueous solution (0.5 M, pH = 7) of bare and C-doped TiO_2 under simulated sunlight at 0 V.

In our case we fixed the cycles of illumination at 20 seconds, this period of time should permit to reach a stable current and hence to reach the equilibrium between the two opposite processes. Studying the current decay profile, it is possible to get an idea of the electron-hole pairs production and recombination mechanisms. The photocurrent density produced by the C-doped titania electrode reached 510 μA cm^{-2}, much higher than that measured on TiO_2 films (Figure 8). This improvement has to be underlined, even if this photocurrent value can be considered as relatively weak, probably due to inappropriate back contact resistance.

3.4 Photovoltaic investigation in DSSC.

The new titanium oxide pastes, with increasing amount of carbon dopant, have been investigated and the photovoltaic parameters have been reported in Table 1, as well as the *J/V* curves of the devices in Figure 9a and 9b, respectively. The doped TiO_2 paste, named as TiO_2-C followed by a number that represent the percentage of C-dopant, have been compared with the commercial analogous paste (Solaronix T/SP) and with a paste prepared using pure anatase-TiO_2 (TiO_2-A), that is the same used to prepare the doped systems. Solar devices were prepared using either a single layer film consisting of a transparent 20 nm particles layer (10 μm) of TiO_2 paste and a double in combination with the commercial scattering layer (5 μm, Solaronix R/SP) containing optically dispersing anatase > 100 nm particles. The liquid electrolyte **A6141** (0.6 M *N*-butyl-*N*-methyl imidazolium iodide, 0.03 M I_2, 0.10 M guanidinium thiocyanate, and 0.5 M 4-*t*-butylpyridine in acetonitrile/valeronitrile 85:15)[49, 50] was used for testing the photovoltaic properties of devices. In addition, we have investigated the photovoltaic in presence of equimolar amount of

chenodeoxycholic acid (CDCA) as a de-aggregating co-adsorbent agent[51] in the sensitizer solution (CDCA:dye = 1:1). The highest recorded efficiency in these measurements has been achieved with the commercial paste in both configurations, single and double layer. The interesting fact is that the photocurrent is slightly higher compared to the titania paste prepared using TiO_2 nanoparticles, but the photovoltage is 80 mV lower. The values recoded for the home-made titania pastes are similar except for the best samples C24 which has allowed to record a PCE value almost equal to the commercial best paste both in case of single- or double-layer devices. This is obviously due to the carbon doping, in fact, the cells made with the pure anatase-TiO_2 used as reference, showed a lower efficiency. Whereas the cells use the same sensitizer, it is meaningless to analyse the IPCE characteristic, but it is more significant to consider the electrochemical characteristics and the dye loading.

The dye loading has been ascertained via optical absorption of a proper solution of the desorbed dyes from the photoanode as described in our previous works.[42] The results are reported in Table 1 and graphically depicted in Figure 10.

Table 1. Photovoltaic characteristics and dye loading of DSSCs containing C-doped TiO_2 films and comparison with commercials TiO_2 pastes. (Value without mask are in brackets)

Device[a]	J_{sc}		V_{oc}		FF		PCE		Dye adsorbed
	[mA cm^{-2}]		[mV]		[%]		[%]		[10^{-8} mol cm^{-2}]
Solaronix T/SP-R/SP[b]	15.6	(17.9)	720	(722)	72	(71)	8.1	(9.2)	15.9
Solaronix T/SP[c]	15.4	(15.7)	732	(758)	73	(75)	8.2	(8.9)	11.9
TiO_2-A[c]	11.9	(13.6)	802	(780)	76	(75)	7.3	(7.9)	6.9
TiO_2-A + Solaronix R/SP[b]	11.5	(13.0)	758	(760)	74	(73)	6.4	(7.2)	6.5
TiO_2-C24[c]	11.3	(14.5)	792	(797)	76	(74)	6.8	(8.5)	5.5
TiO_2-C24 + Solaronix R/SP[b]	13.2	(15.7)	778	(785)	75	(74)	7.7	(9.1)	6.3
TiO2-C32[c]	11.6	(13.5)	775	(778)	73	(74)	6.6	(7.8)	6.4
TiO_2-C32 + Solaronix R/SP[b]	11.7	(14.0)	778	(781)	76	(75)	6.9	(8.2)	5.9
TiO_2-C40[c]	10.9	(12.1)	778	(778)	76	(75)	6.4	(7.1)	5.3
TiO_2-C40 + Solaronix R/SP[b]	10.9	(11.9)	762	(775)	75	(75)	6.2	(6.9)	6.1

[a] Dye solution of 5 x 10-4 M in EtOH solution with 1:1 CDCA; electrolyte A6141 (0.6 M N-butyl-N-methyl imidazolium iodide, 0.03 M I_2, 0.10 M guanidinium thiocyanate, and 0.5 M 4-t-butylpyridine in acetonitrile/valeronitrile 85:15; [b] Double TiO_2 layer (10+5 μm); [c] Single TiO_2 layer (10 μm);[d] surface area 0.20 cm^2

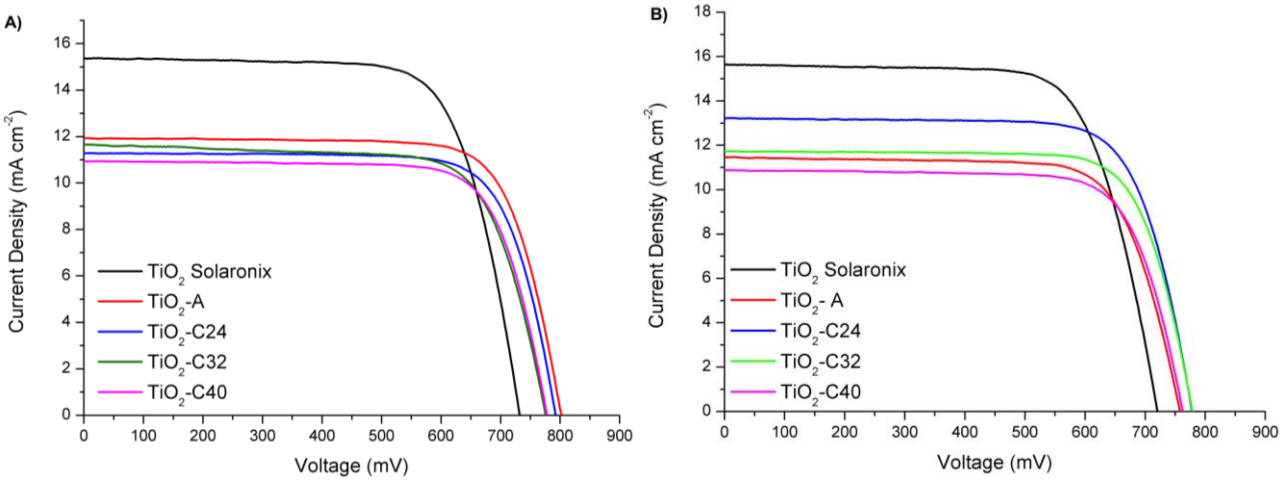

Figure 9. *J–V* characteristics of (a) single layer and (b) double layers DSCs containing carbon-doped TiO_2 films and comparison with commercials TiO_2 pastes. (full AM 1.5G solar intensity).

The significant fact that emerges from this series of measurements is that the titania prepared from nanoparticles of anatase-TiO_2 absorbs a significantly lower amount (about 50% less) of dye than that prepared from commercial pastes. Though it is not known the exact composition of the commercial pastes, what appears evident simply depositing them to prepare photoanodes, it is that are much more transparent compared with those prepared from nanoparticles. This is definitely related to scattering phenomena due to the formation of large aggregates in the pastes prepared from nanoparticles compared to the commercial. In other words, it is conceivable that the commercial pastes are prepared with nanoparticles of titanium dioxide functionalized for better remain dispersed in the organic environment that form the dough used to prepare the photoanodes, and to remain more transparent after the thermal treatments. In fact, the commercial paste Solaronix T/SP allows to realize devices with a high degree of transparency, which is impossible using the pastes prepared using bare TiO_2 nanoparticles. This effect could be considered negative in the case of devices used in smart windows (i.e. photovoltaic windows). However, if the devices are made as a double layer in combination with a scattering layer, this becomes meaningless. The formation of large aggregates can also explain such a substantial difference in the amount of absorbed dye. To get a clearer idea of such phenomena are at the basis of the different absorption of the dye it will be necessary to study the surface area and the porosity of the titania powder obtained from the different studied pastes. This will allow us to determine whether the difference in dye loading is due to a different morphology or other phenomena not yet taken into account.

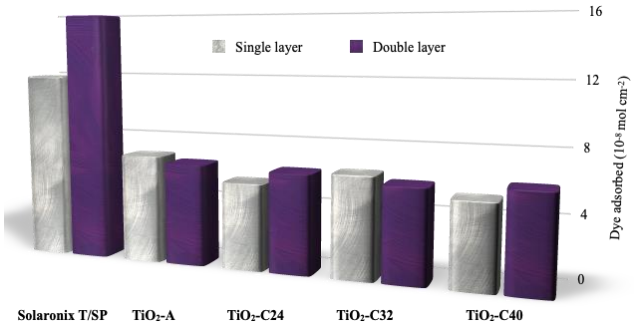

Figure 10. Comparison of dye adsorbed on single layer (gray pattern) and double layer (purple pattern) DSCs containing C-doped TiO_2 films and comparison with commercials TiO_2 pastes.

However, it is possible an analysis of the electrical phenomena that occur within the devices made with the different pastes going to study the devices themselves by means of electrochemical impedance spectroscopy (EIS). The Nyquist plots (Figure 11a and b) show the characteristic feature of DSSC spectra. The electrochemical charge transfer process at the Pt electrode and the electron leaking at the photoanode/electrolyte interface correspond the high, and low frequency semicircles, respectively. Data were fitted using the equivalent circuit model shown in the inset of Figure 9b, the corresponding electrochemical parameters are reported in Table 2.

Table 2. Impedance characteristics of single- and double-layers DSCs containing carbon-doped TiO2 films and comparison with commercials TiO_2 pastes, with a commercial TiO_2 scattering layer.

Device[a]	R_{rec}	$C_{dl,Pt}$ x10^4	τ
	[Ω]	[F]	[ms]
Solaronix T/SP-R/SP	8.0	7.6	6.1
Solaronix T/SP	11	3.9	4.3
TiO_2-A	12	3.2	3.7

TiO_2-A + Solaronix R/SP	11	3.8	4.3
TiO_2-C24	16	2.5	4.0
TiO_2-C24 + Solaronix R/SP	13	3.6	4.3
TiO_2-C32	16	2.7	4.3
TiO_2-C32 + Solaronix R/SP	12	3.5	4.2
TiO_2-C40	12	3.5	4.1
TiO_2-C40 + Solaronix R/SP	11	3.7	4.3

Since we are interested in the effect of the carbon doping of titania on the cell performances, we will focus the attention only on the high frequency semicircle which depends on the interfacial feature of the titania/electrolyte inter-phase. The electron time life in the titania appears to be correlated to the quantity of adsorbed dye: the larger the amount of dye the longest the electron time life.
Moreover, the decrease in electron time life does not depend from the recombination resistance while is mostly affected by the decrease of double layer capacitance; indeed, the dielectric permittivity of the interface is lower in sample with less amount of the neutral organic molecule onto the semiconductor surface.
Though the reasons why the efficiency values recorded by the devices prepared using the C-doped-TiO_2 are not yet completely understood, it is clear that their use can have a very positive effect on the final performance. Furthermore, the use of these pastes could be particularly interesting especially in double layer devices. In fact, in case the transparency of the device is not a requirement of primary importance, the use of these pastes allows us to drastically reduce the amount of dye per unit area, thus reducing costs and allowing us to also use the high-performance dyes whose synthesis may be long and costly.

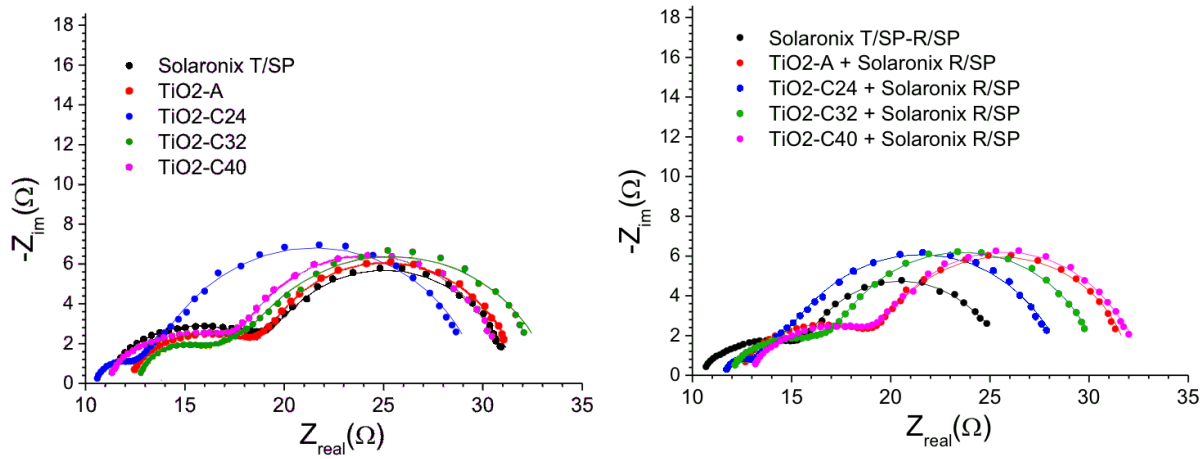

Figure 11. Nyquist plots of (a) single layer and (b) double layers DSCs containing carbon-doped TiO_2 films and comparison with commercials TiO_2 pastes. Dot points: experimental data; continuous line: fitted data.

4. CONCLUSIONS

A green approach based on a simple "multi-step" mild process to easily produce carbon doped TiO_2, have been successfully described. DSSCs produced by C-doped samples showed increased visible light absorption, allowing to reach a solar energy conversion efficiency almost equal to the commercial with greater open-circuit voltage and greater than efficiency obtained with conventional TiO_2 nanoparticles. Moreover, the C-doped devices are sensitized with a smaller amount of dyes that can lower the final cost of the device. Therefore, the new C-doped titania is an attractive component for faster industrial realization of solar devices due to a significant reduction of cost, ease of scaling up, and improved performances.

AUTHOR INFORMATION

Corresponding Author

* Alessandro Abbotto, email: alessandro.abbotto@unimib.it
* Giovanna Brusatin, email: giovanna.brusatin@unipd.it
* Norberto Manfredi, email: norberto.manfredi@unimib.it

Present Addresses

Author Contributions

The manuscript was written through contributions of all authors. / All authors have given approval to the final version of the manuscript.

Funding Sources

This work was carried out under financial support from MIUR (grant Dipartimenti di Eccellenza - 2017 "Materials for Energy") and University of Milano-Bicocca (Fondo di Ateneo - Quota Competitiva 2017 and 2019). RM, SC, GB and FM acknowledge the Università Italo-Francese for the financial funding through the Galileo project n° 28143XK.

ACKNOWLEDGMENT

Dr Philippe Decorse for technical support for XPS measurements.

R.R., A.A., and N.M. wish to acknowledge the Ministero dell'Università e della Ricerca (MIUR) and University of Milano-Bicocca for the financial support.

REFERENCES

[1] B. O'Regan, M. Gratzel, Nature, 353 (1991) 737-740.

[2] IDTechEx Research report "Dye Sensitized Solar Cells (DSSC/DSC) 2013–2023: Technologies, Markets, Players" (www.IDTechEx.com/dssc)

[3] S. Mozaffari, M.R. Nateghi, M.B. Zarandi, Renew. Sustain. Energy Rev., 71 (2017) 675-686.

[4] J. Wu, Z. Lan, J. Lin, M. Huang, Y. Huang, L. Fan, G. Luo, Chem Rev, 115 (2015) 2136-2173.

[5] U. Ahmed, M. Alizadeh, N.A. Rahim, S. Shahabuddin, M.S. Ahmed, A.K. Pandey, Sol. Energy, 174 (2018) 1097-1125.

[6] B. Boro, B. Gogoi, B.M. Rajbongshi, A. Ramchiary, Renew. Sustain. Energy Rev., 81 (2018) 2264-2270.

[7] A. Carella, F. Borbone, R. Centore, Front. Chem., 6 (2018).

[8] N. Roslan, M.E. Ya'acob, M.A.M. Radzi, Y. Hashimoto, D. Jamaludin, G. Chen, Renew. Sustain. Energy Rev., 92 (2018) 171-186.

[9] A.A. Mohamad, Sol. Energy, 190 (2019) 434-452.

[10] M. Pelaez, N.T. Nolan, S.C. Pillai, M.K. Seery, P. Falaras, A.G. Kontos, P.S.M. Dunlop, J.W.J. Hamilton, J.A. Byrne, K. O'Shea, M.H. Entezari, D.D. Dionysiou, Appl. Catal., B-Environ, 125 (2012) 331-349.

[11] S. Afzal, W.A. Daoud, S.J. Langford, ACS Appl. Mater. Interfaces, 5 (2013) 4753-4759.

[12] S.-H. Wu, J.-L. Wu, S.-Y. Jia, Q.-W. Chang, H.-T. Ren, Y. Liu, Appl. Surf. Sci., 287 (2013) 389-396.

[13] S.N.R. Inturi, T. Boningari, M. Suidan, P.G. Smirniotis, Appl. Catal., B-Environ, 144 (2014) 333-342.

[14] N. Serpone, D. Lawless, J. Disdier, J.-M. Herrmann, Langmuir, 10 (1994) 643-652.

[15] Z. Yao, M. Zhang, H. Wu, L. Yang, R. Li, P. Wang, J. Am. Chem. Soc., 137 (2015) 3799-3802.

[16] K. Kakiage, Y. Aoyama, T. Yano, K. Oya, J.-i. Fujisawa, M. Hanaya, Chem. Commun., 51 (2015) 15894-15897.

[17] N. Serpone, J. Phys. Chem. B, 110 (2006) 24287-24293.

[18] R. Asahi, T. Morikawa, T. Ohwaki, K. Aoki, Y. Taga, Science, 293 (2001) 269-271.

[19] V.N. Kuznetsov, N. Serpone, J. Phys. Chem. B, 110 (2006) 25203-25209.

[20] S. Banerjee, S.C. Pillai, P. Falaras, K.E. O'Shea, J.A. Byrne, D.D. Dionysiou, J. Phys. Chem. Lett., 5 (2014) 2543-2554.

[21] S. Sakthivel, H. Kisch, Angew. Chem. Int. Ed., 42 (2003) 4908-4911.

[22] R. Taziwa, E.L. Meyer, E. Sideras-Haddad, R.M. Erasmus, E. Manikandan, B.W. Mwakikunga, Int J Photoenergy, 2012 (2012) 9.

[23] I. Hiroshi, W. Yuka, H. Kazuhito, Chem. Lett., 32 (2003) 772-773.
[24] S.H. Kang, H.S. Kim, J.-Y. Kim, Y.-E. Sung, Mater. Chem. Phys., 124 (2010) 422-426.
[25] R. Kushwaha, R. Chauhan, P. Srivastava, L. Bahadur, J. Solid State Electrochem., 19 (2015) 507-517.
[26] H. Diker, C. Varlikli, E. Stathatos, Int. J.Energy Res., 38 (2014) 908-917.
[27] X. Chen, C. Burda, J. Am. Chem. Soc., 130 (2008) 5018-5019.
[28] I.N. Martyanov, S. Uma, S. Rodrigues, K.J. Klabunde, Chem. Commun., (2004) 2476-2477.
[29] G. Wu, T. Nishikawa, B. Ohtani, A. Chen, Chem. Mater., 19 (2007) 4530-4537.
[30] M. Shen, Z. Wu, H. Huang, Y. Du, Z. Zou, P. Yang, Mater. Lett., 60 (2006) 693-697.
[31] C.-S. Kuo, Y.-H. Tseng, C.-H. Huang, Y.-Y. Li, J. Mol. Catal. A: Chem., 270 (2007) 93-100.
[32] Y. Park, W. Kim, H. Park, T. Tachikawa, T. Majima, W. Choi, Appl. Catal., B-Environ, 91 (2009) 355-361.
[33] Y. Huang, W. Ho, S. Lee, L. Zhang, G. Li, J.C. Yu, Langmuir, 24 (2008) 3510-3516.
[34] A. Lin, D. Qi, H. Ding, L. Wang, M. Xing, B. Shen, J. Zhang, Catal. Today, 281 (2017) 636-641.
[35] S.K. Park, J.S. Jeong, T.K. Yun, J.Y. Bae, J Nanosci Nanotechno, 15 (2015) 1529-1532.
[36] R. Taziwa, E. Meyer, Advances in Nanoparticles, 3 (2014) 54-63.
[37] A. Colombo, C. Dragonetti, D. Roberto, R. Ugo, N. Manfredi, P. Manca, A. Abbotto, G. Della Giustina, G. Brusatin, Inorg. Chim. Acta, 489 (2019) 263-268.
[38] F. Dong, S. Guo, H. Wang, X. Li, Z. Wu, J. Phys. Chem. C, 115 (2011) 13285-13292.
[39] S. Ito, T.N. Murakami, P. Comte, P. Liska, C. Grätzel, M.K. Nazeeruddin, M. Grätzel, Thin Solid Films, 516 (2008) 4613-4619.
[40] S. Ito, P. Chen, P. Comte, M.K. Nazeeruddin, P. Liska, P. Péchy, M. Grätzel, Progr. Photovolt: Res. Appl., 15 (2007) 603-612.
[41] C. Baldoli, S. Bertuolo, E. Licandro, L. Viglianti, P. Mussini, G. Marotta, P. Salvatori, F. De Angelis, P. Manca, N. Manfredi, A. Abbotto, Dyes Pigm., 121 (2015) 351-362.
[42] E. Dell'Orto, L. Raimondo, A. Sassella, A. Abbotto, J. Mater. Chem., 22 (2012) 11364-11369.
[43] D. Dova, S. Cauteruccio, N. Manfredi, S. Prager, A. Dreuw, S. Arnaboldi, P.R. Mussini, E. Licandro, A. Abbotto, Dyes Pigm., 161 (2019) 382-388.
[44] S. Chaguetmi, F. Mammeri, M. Pasut, S. Nowak, H. Lecoq, P. Decorse, C. Costentin, S. Achour, S. Ammar, J. Nanopart. Res., 15 (2013) 2140.
[45] F. Fabregat-Santiago, J. Bisquert, G. Garcia-Belmonte, G. Boschloo, A. Hagfeldt, Sol. Energy Mater. Sol. Cells, 87 (2005) 117-131.
[46] N. Manfredi, V. Trifiletti, F. Melchiorre, G. Giannotta, P. Biagini, A. Abbotto, New J. Chem., 42 (2018) 9281-9290.
[47] K. Szot, M. Rogala, W. Speier, Z. Klusek, A. Besmehn, R. Waser, Nanotechnology, 22 (2011) 254001.
[48] N.J. Bell, Y.H. Ng, A. Du, H. Coster, S.C. Smith, R. Amal, J. Phys. Chem. C, 115 (2011) 6004-6009.
[49] M.K. Nazeeruddin, F. De Angelis, S. Fantacci, A. Selloni, G. Viscardi, P. Liska, S. Ito, B. Takeru, M. Grätzel, J. Am. Chem. Soc., 127 (2005) 16835-16847.
[50] F. Fabregat-Santiago, G. Garcia-Belmonte, I. Mora-Sero, J. Bisquert, Phys. Chem. Chem. Phys., 13 (2011) 9083-9118.
[51] T. Marinado, M. Hahlin, X. Jiang, M. Quintana, E.M.J. Johansson, E. Gabrielsson, S. Plogmaker, D.P. Hagberg, G. Boschloo, S.M. Zakeeruddin, M. Grätzel, H. Siegbahn, L. Sun, A. Hagfeldt, H. Rensmo, J. Phys. Chem. C, 114 (2010) 11903-11910.